Journal of Chromatography A 1652 (2021) 462358

Contents lists available at ScienceDirect

Journal of Chromatography A

journal homepage: www.elsevier.com/locate/chroma

Baseline correction method for dynamic pressure gradient modulated comprehensive two-dimensional gas chromatography with flame ionization detection

Lina Mikaliunaite, Paige E. Sudol, Caitlin N. Cain, Robert E. Synovec*

Department of Chemistry, University of Washington, Box 351700, Seattle, WA 98195, USA

ARTICLE INFO

Article history:
Received 12 April 2021
Revised 16 June 2021
Accepted 17 June 2021
Available online 26 June 2021

Keywords:
Comprehensive two-dimensional gas chromatography
dynamic pressure gradient modulation
flame ionization detection
trace analysis
baseline correction method

ABSTRACT

A baseline correction method is developed for comprehensive two-dimensional (2D) chromatography (GC × GC) with flame-ionization detection (FID) using dynamic pressure gradient modulation (DPGM). The DPGM-GC × GC-FID utilized porous layer open tubular (PLOT) columns in both dimensions to focus on light hydrocarbon separations. Since DPGM is nominally a stop-flow modulation technique, a rhythmic baseline disturbance is observed in the FID signal that cycles with the modulation period (P_M). This baseline disturbance needs to be corrected to optimize trace analysis. The baseline correction method has three steps: collection of a background "blank" chromatogram and multiplying it by an optimized normalization factor, subtraction of the normalization-optimized background chromatogram from a sample chromatogram, and application of Savitzky-Golay smoothing. An alkane standard solution, containing pentane, hexane and heptane was used for method development, producing linear calibration curves ($r^2 > 0.991$) over a broad concentration range (7.8 ppm – 4000 ppm). Further, the limit-of-detection (*LOD*) and limit-of-quantification (*LOQ*) were determined for pentane (*LOD* = 2.5 ppm, *LOQ* = 8.2 ppm), hexane (*LOD* = 0.9 ppm, *LOQ* = 3.0 ppm), and heptane (*LOD* = 1.9 ppm, *LOQ* = 6.4 ppm). A natural gas sample separation illustrated method applicability, whereby the DPGM produced a signal enhancement (*SE*) of 30 for isopentane, where *SE* is defined as the height of the tallest ^{2}D peak in the modulated chromatogram for the analyte divided by the height of the unmodulated ^{1}D peak. The 30-fold *SE* resulted in about a 10-fold improvement in the signal-to-noise ratio (*S/N*) for isopentane. Additional versatility of the baseline correction method for more complicated samples was demonstrated for an unleaded gasoline sample, which enabled the detection (and visual appearance) of trace components.

1. Introduction

Low molecular weight and low boiling point compounds, commonly referred to as volatile organic compounds (VOCs), are critical components in a variety of samples of analytical interest, such as wastewater [1,2], soil [3,4], natural gas [5], and gasoline [6–8]. Since these compounds can often be present at trace levels (i.e., low ppm range), they require analysis via sensitive and robust analytical instrumentation. Natural gas is a particularly challenging sample matrix, as it contains primarily methane as well as longer and much less volatile hydrocarbons ranging from C6 to C12 [9–12].

Gas chromatography (GC) is the prominent technique for the detection and quantification of VOCs due to the high selectivity and resolution provided [1,2,4]. Method development for GC analysis of VOCs primarily relies upon the appropriate selection of the separation column. Primarily, GC separations are performed using wall-coated open tubular (WCOT) capillary columns, where a film of a liquid stationary phase is directly coated on the inside of the capillary. WCOT columns provide more efficient separations compared to packed columns [13]. However, very low molecular weight VOCs can exhibit poor retention on packed columns [14,15] or WCOT columns [16] due to the extreme volatility which causes them not to be baseline separated. In contrast, porous layer open tubular (PLOT) columns can be used for better separation of highly volatile, low molecular weight VOCs, as they provide unique selectivity and suitable retention for these compounds. PLOT columns utilize a layer of a porous adsorbent like fused silica, alumina, or molecular sieves to coat the inner wall of the capillary column [13]. For example, Burger et al. recently developed a cryo-wafer device containing multiple PLOT capillary columns for headspace sampling of the C6+ fraction of natural gas, followed by desorp-

* Corresponding author.
E-mail address: synovec@chem.washington.edu (R.E. Synovec).

https://doi.org/10.1016/j.chroma.2021.462358
0021-9673/

tion into a GC-MS for identification and relative quantification [17]. While PLOT columns improve the retention of these low molecular weight VOCs, coelution of isomers and a low signal-to-noise ratio (*S/N*) can still complicate the analysis.

However, the use of comprehensive two-dimensional (2D) gas chromatography (GC × GC) can overcome these challenges by providing an orthogonal separation dimension and improving signal enhancement [18–20]. GC × GC was introduced by Liu and Philips [21], and has evolved ever since with wide applicability in many different fields like forensics [22], cosmetics [23,24] environmental science [25,26], and food analysis [27]. In GC × GC, the first-dimension (^{1}D) column is coupled to a second-dimension (^{2}D) column by a modulator, which nominally isolates and reinjects the ^{1}D eluate onto the ^{2}D column [28,29]. GC × GC can provide about a 10-fold increase in peak capacity relative to one-dimensional GC [30], as well as considerable signal enhancement. Generally, thermal modulators provide the greatest signal enhancement in GC × GC work as a result of the temperature differential utilized to trap and reinject analytes, which produces a 100% duty cycle (i.e., all of the ^{1}D eluate is transferred to the ^{2}D column) [31–34]. Thermal modulators have been used in conjunction with PLOT columns in GC × GC, and although they are widely commercially available, some are expensive to operate due to requiring liquid nitrogen, making them largely impractical in certain scenarios, and others (consumable-free) have limited performance to modulate the lightest and most volatile analytes [35,36]. Conversely, flow modulators utilize a redirection of gas flow to transfer eluate from the ^{1}D to ^{2}D column [37–43]. Flow modulators have become more commercially accessible in recent years and are less costly due to not requiring cryogens, making them a more feasible option for small-scale applications. However, while commercial flow modulators, like the Agilent G3486A CFT, have been successfully used with PLOT columns in both dimensions [44,45], these are flow diversion modulators, that may require high flow rates on second dimension [29], that in turn may limit applicability of PLOT columns. Many flow modulators utilize a waste port, with resulting duty cycles of only approximately 10 to 40% [38,46–48]. Thus, some commercial flow modulators may not be ideal for the trace analysis of low molecular weight VOCs via GC × GC, which would benefit from utilization of a full-transfer (100% duty cycle) [29,42,43] flow modulation technique such as dynamic pressure gradient modulation (DPGM) [41–43].

Herein, we demonstrate the capability of DPGM towards the trace analysis of lightweight VOCs in natural gas and gasoline samples. A reverse GC × GC column configuration is utilized, with a polar PLOT-BOND ^{1}D column and a non-polar PLOT-Q ^{2}D column. DPGM operates by applying an auxiliary gas pressure (P_{aux}) to a T-union, which joins the ^{1}D and ^{2}D columns, in a cyclic rhythm based on the modulation period (P_M) and pulse width (p_w) [41]. During the P_M, a suitable P_{aux} is first applied to the T-union to temporarily stop the flow of the ^{1}D eluate to the ^{2}D column. Then, P_{aux} is turned off for a time interval (p_w), allowing for the ^{1}D eluate to pass through the T-union before P_{aux} is reapplied, which rapidly reinjects the ^{1}D eluate onto the ^{2}D column; this process repeats so all ^{1}D eluate for each P_M enters the ^{2}D column in a rapid pulse [41]. Previous work has demonstrated DPGM, can be used for a short P_M, provide full modulation (100 % duty cycle) and signal enhancement (*SE*) between 7 and 87 depending on the compound, where the *SE* is the ratio of the highest ^{2}D peak relative to the unmodulated ^{1}D peak [18–20,41]. Application of DPGM not only provides a high *SE* that benefits the detectability of trace compounds, but also more efficient ^{2}D separations are provided due to the production of narrow ^{2}D peaks which results in an increased in peak capacity [30]. As a stop-flow modulation technique [41], DPGM introduces a rhythmic baseline disturbance (as a function of the P_M) that is subsequently observed in the FID [47,49]. While these baseline disturbances have been noted in the literature [50,51], a data analysis method to correct for these baseline signal disturbances to facilitate accurate peak quantification (especially for trace analysis) has not been developed and investigated until now.

Therefore, in demonstrating the performance of DPGM for trace analysis, herein we develop a baseline correction method for GC × GC-FID using DPGM, referred to as DPGM-GC × GC-FID. Performance of this method will be evaluated by generating calibration curves for standard solutions containing three alkanes (pentane, hexane, and heptane) along with analyzing natural gas and gasoline samples. The baseline correction method will be shown to substantially extend the calibration and quantification down to the single digit ppm range.

2. Experimental

All experiments were performed using DPGM-GC × GC-FID, which is based upon an Agilent 6890 GC (Agilent Technologies, Palo Alto, CA, USA) with FID as shown in Fig. 1A. The stock electrometer for the Agilent FID was replaced by an in-house built electrometer that allows data to be collected at 100 kHz, with the data boxcar averaged to 1 kHz. The electrometer was interfaced to a data acquisition board and the data was collected using an in-house program written in LabVIEW (National Instruments, Austin, TX, USA). Post-run data processing was performed in MATLAB R2020a (The Mathworks, Inc., Natick, MA, USA).

A reverse GC × GC column configuration was utilized with a polar ^{1}D column (Silica BOND PLOT, 30 m × 320 μm d_c, Restek Corporation, Bellefonte, PA, USA) and a non-polar ^{2}D column (PLOT-Q, 2 m × 250 μm d_c, Restek, Bellefonte Corporation, PA, USA). For consistency, this PLOT column configuration was used for all experiments. Constant volumetric flowrates of 1.3 ml/min and 3.9 ml/min were applied to the ^{1}D and ^{2}D columns, respectively. To implement DPGM, the ^{1}D and ^{2}D capillary GC columns were connected using a 3-way T-union (Model MT.5CXS6, Valco Instruments Company Inc., Houston, TX, USA), with the third port connected to a high-speed pulse valve (Model 009-0347-900, Parker Hannifin, Hollis, NH). Connection was achieved using a specialized fitting and a 5 cm × 125 μm i.d. stainless steel transfer line (VICI model T5C5D, Valco Instruments Company Inc., Houston, TX, USA). The pulse valve was controlled using the same previously mentioned LabVIEW program.

Initially, background chromatogram runs were obtained using P_M = 6 s with p_w = 2 s, where p_w is the time interval in which the pulse valve flow is shut off per each P_M. Ultra-high purity hydrogen (Grade 5 99.999%, Praxair, Seattle, WA, USA) was used as the carrier gas that was additionally filtered using a triple gas filter (Restek Corporation, Bellefonte, PA, USA), designed to remove oxygen, moisture, and hydrocarbons. The temperature was ramped from 200 °C to 250 °C at 10 °C/min and held for 7 min, to ensure equilibration of temperature in the oven. All pressure ramp tuning for DPGM implementation was achieved as previously described [41]. The inlet pressure was ramped from 37.9 kPa (5.5 psig) to 44.1 kPa (6.4 psig) at the rate of 1.2 kPa/min (0.18 psig/min). Auxiliary pressure, P_{aux}, (i.e., independent hydrogen flow from the pulse valve) was ramped from 29.6 kPa (4.3 psig) to 34.5 kPa (5 psig) at the rate of 1 kPa/min (0.14 psig/min). The inlet and FID were set to a constant temperature of 250 °C for all experiments herein. Additionally, acetone (solvent) background runs, and background runs without sample or solvent injection, were collected at the same P_M = 6 s and p_w = 2 s one right after another (4 replicates each), to determine if the solvent influences the detected background.

A stock alkane standard solution of 20,000 ppm containing pentane, hexane, and heptane at equal concentrations (diluted in acetone) was used to develop the baseline correction method. The stock solution was diluted in acetone to create standard solutions

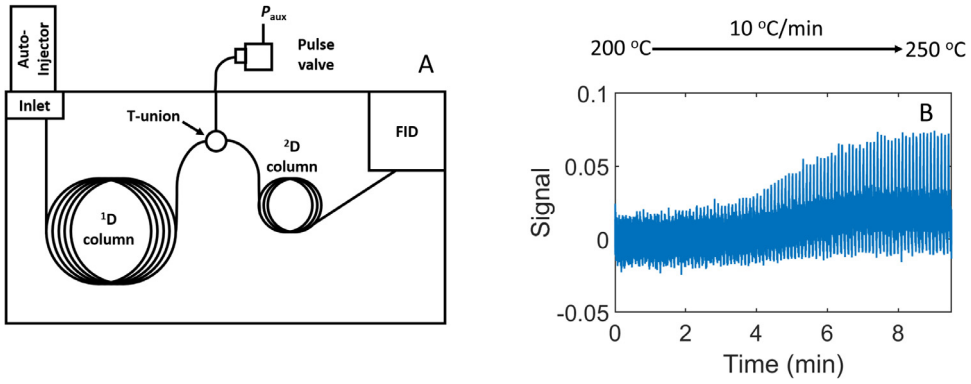

Fig. 1. (A) Schematic of the major components of DPGM-GC × GC-FID instrument. A pulse valve provides dynamic pressure gradient modulation (DPGM) between the ^{1}D and ^{2}D columns, at the T-union by applying a suitable pressure (P_{aux}). Detection was performed with a flame ionization detector (FID). (B) Background chromatogram collected with the temperature program from 200 °C to 250 °C at 10 °C /min.

of 4000, 2000, 1000, 500, 250, 125, 62.5, 31.3, 15.6 and 7.8 ppm concentration. Sample injection was carried out using a 7683B auto-injector (Agilent Technologies, Palo Alto, CA, USA). A 0.1 μl of sample was injected without a split, for better reproducibility when quantifying the areas, and all chromatograms were acquired in quadruplicate. To reduce wraparound, a P_M = 6 s and a pulse width, p_w, of 2 s were utilized. The temperature of the GC oven was held at 200 °C and ramped after injection using a temperature program of 10 C/min to 250 °C, where it was held for 7 min. The inlet pressure was ramped from 37.9 kPa (5.5 psig) to 44.1 kPa (6.4 psig) at the rate of 1.2 kPa/min (0.18 psig/min). Auxiliary pressure, P_{aux}, was ramped from 29.6 kPa (4.3 psig) to 34.5 kPa (5 psig) at the rate of 1 kPa/min (0.14 psig/min).

Analysis of a natural gas sample (Air Liquide, Paris, France) containing n-butane (3%), carbon dioxide (1%), ethane (9%), helium (0.5%), isobutane (3%), isopentane (1%), nitrogen (5%), *n*-pentane (1%) and propane (6%) in methane illustrated applicability of the baseline correction method for compositional analysis of environmental samples. A 50 μl sample was collected from the gas cylinder and manually injected, and optimal modulation conditions to reduce wraparound were utilized: P_M = 2 s, p_w = 0.55 s. The GC oven temperature was ramped from 100 °C to 150 °C at a rate of 10 °C/min, then ramped from 150 °C to 200 °C at a rate of 20 °C/min, and finally held at 200 °C for 5 min. The inlet pressure was first ramped from 26.9 kPa (3.9 psig) to 32.4 kPa (4.7 psig) at the rate of 1.1 kPa/min (0.16 psig/min), then ramped to 37.9 kPa (5.5 psig) at a rate of 2.2 kPa/min (0.32 psig/min). Auxiliary pressure, P_{aux}, was first ramped from 20.7 kPa (3.0 psig) to 24.8 kPa (3.6 psig) at the rate of 0.8 kPa/min (0.12 psig/min), then to 29.6 kPa (4.3 psig) at a rate of 1.9 kPa/min (0.28 psig/min).

Unleaded gasoline sourced from a local gas station was analyzed to show the versatility of the separation and baseline correction methods while using a more complex sample. A 0.1 μl sample was injected in split-less mode. The analysis was performed at two different sets of modulation conditions, (1) P_M = 2 s, p_w = 0.5 s and (2) P_M = 6 s, p_w = 2 s, to illustrate both full utilization of the 2D separation space (P_M = 2 s) and minimal wraparound (P_M = 6 s). The oven temperature was ramped from 120 °C to 230 °C at 10 °C/min, then from 230 °C to 250 °C at 20 °C/min, and finally held constant at 250 °C for 30 min. The inlet pressure was first ramped from 29.0 kPa (4.2 psig) to 41.4 kPa (6 psig) at the rate of 1.1 kPa/min (0.16 psig/min), then ramped to 44.1 kPa (6.4 psig) at a rate of 2.8 kPa/min (0.4 psig/min). Auxiliary pressure, P_{aux}, was first ramped from 22.1 kPa (3.2 psig) to 32.4 kPa (4.7 psig) at the rate of 1.0 kPa/min (0.14 psig/min), then to 34.5 kPa (5 psig) at a rate of 2.1 kPa/min (0.3 psig/min).

3. Results and discussion

When using the DPGM-GC × GC-FID instrument (Fig. 1A), the background exhibited a repetitive signal pattern that increased in intensity along the ^{1}D separation, due to the stop-flow nature of using DPGM during the temperature program at constant flow through each of the columns (Fig. 1B). The most likely source of the repetitive signal pattern disturbance observed in the baseline is the flow fluctuations inherit to DPGM in conjunction with either the potential for organic compound impurities in the carrier gas or the injected acetone solvent used in sample preparation. To study the acetone solvent possibility, acetone blanks and instrument background blanks (program started using the autoinjector, but without a sample or solvent injected) were run in pairs one right after another four times in total (Fig. 2A–D). In blue, the acetone blank is shown, and in red, the instrument background is shown. In black, the subtraction of instrument background from the acetone blank is presented. The small differences indicate that the backgrounds vary slightly run-to-run, however there is also slight variation between the acetone and instrument blanks. Note that for the acetone blank runs, the large acetone peak has observed at ~ 10 min, off-scale to the right in Fig. 2A–D. To examine the possibility of organic compounds in the carrier gas, we performed background runs after changing the carrier gas filter, from the initial filter to a new one, as the FID acts as a quasi-mass flow meter, which would have more ionizable atoms reaching it per unit time when the flow increases if the carrier gas contains organic compound impurities. No difference in the backgrounds was observed after the filter change. This outcome, while not totally conclusive, suggests both filters are likely removing most but not all of the organic compound impurities, and so a sufficient level of the impurities could remain to produce the observed background signal pattern. Moreover, we considered that the noise could be caused by particulate detachment from the PLOT columns during DPGM modulation, and so we repeated blank runs using a WCOT column set for both ^{1}D (CP-WAX 52CB, 30 m × 320 µm d_c × 0.2 µm d_f) and ^{2}D (RTX-5, 2 m × 250 µm d_c × 0.5 µm d_f). The same backgrounds were observed, so the PLOT columns were also dismissed as a cause for the repetitive background noise pattern. Thus, due to this signal pattern in the background, a data processing method is required to mitigate this issue in the analysis of chromatographic separations data using DPGM with the FID.

Development and illustration of the baseline correction method for the 500-ppm standard solution of pentane, hexane, and heptane (diluted in acetone) is presented in Fig. 3. Visual inspection of the 500-ppm standard solution separation in unfolded raw data form (Fig. 3A) shows that the “noise spikes” from the rhythmic

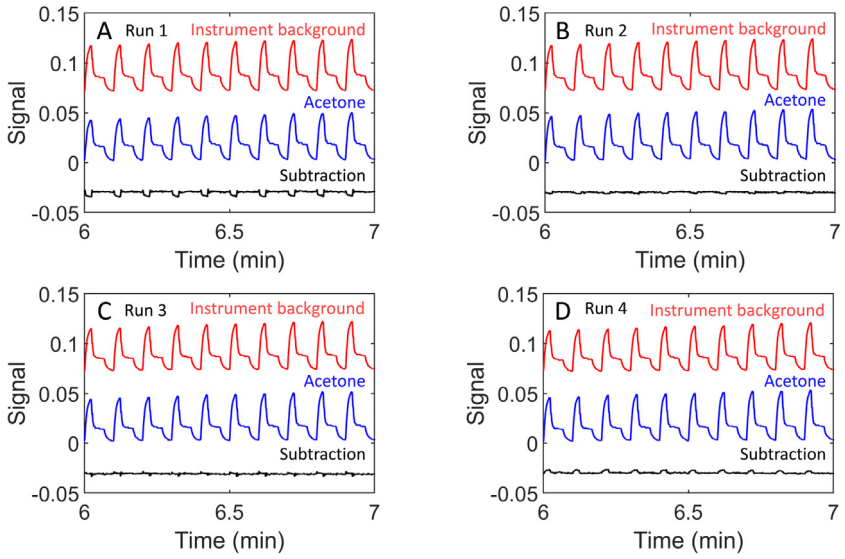

Fig. 2. Background noise for four consecutive runs of solvent (acetone) chromatogram (blue) and instrument background (air injection) chromatogram (red). Subtraction of instrument background from solvent chromatogram is shown in black for runs 1–4. For interpretation of the references to color in this figure legend, the reader is referred to the web version of this article.

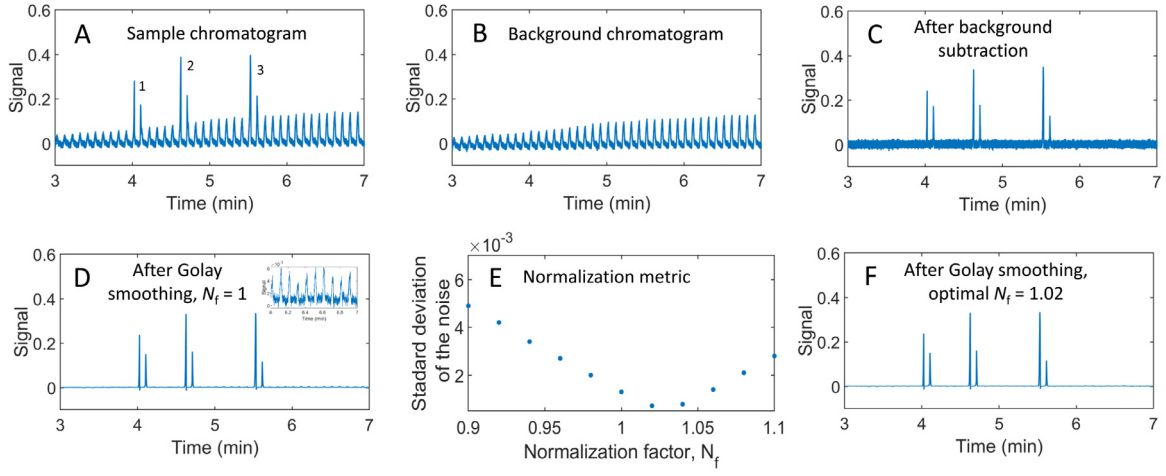

Fig. 3. Demonstration of the baseline correction method. (A) Raw (preprocessed) modulated chromatogram of the 500-ppm alkane standard solution: (1) pentane, (2) hexane and (3) heptane. (B) Raw background chromatogram (no sample injected). (C) Chromatogram after the background subtraction step. (D) Chromatogram after the Savitzky-Golay smoothing step. The insert shows the zoomed-in view of the noise between 6 to 7 min. (E) Standard deviation of the baseline noise in the 6 to 7 min window following background subtraction as a function of the normalization factor (N_f) applied to the background in (B) prior to subtraction. The N_f corresponding to the lowest standard deviation, is the optimized N_f. (F) Fully processed chromatogram when optimized N_f is used (N_f = 1.02).

baseline disturbances, which occur once each P_M, increase during the separation. This observation was reproducible injection-to-injection, if chromatographic conditions were kept constant (eg., the same temperature and flow program is used), illustrating the need for baseline correction. A background chromatogram using the same chromatographic conditions is presented in Fig. 3B. Subtraction of the background chromatogram from the 500-ppm standard solution chromatogram in Fig. 3A is shown in Fig. 3C, where the baseline now appears to be flat in the sense that the noise from the rhythmic baseline disturbances has been essentially eliminated. However, high frequency noise is still present, which is why Savitzky-Golay smoothing is applied to reduce the noise even further; the resulting chromatogram after this data processing step is shown in Fig. 3D. Savitzky-Golay smoothing was performed using a 221 ms time interval for all analyses of the alkane standard solutions. The time interval selected for Savitzky-Golay smoothing was approximately 1/6th the width of a typical ^{2}D peak width (which is 1.3 s), in order to not introduce ^{2}D peak broadening due to this smoothing step. We note that following the Savitsky-Golay smoothing step, the noise spikes from the rhythmic baseline disturbances can still be seen in the baseline, although they are much smaller in magnitude; compare the 6-7 min interval in the background chromatogram of Fig. 3B to the insert in Fig. 3D. This suggests that even though the noise in a given chromatogram (eg., Fig. 3A) is nominally the same as that in a given background chromatogram (Fig. 3B), the reality is that the noise due to the rhythmic baseline disturbances is not sufficiently close to being exactly the same. Therefore, a background normalization step was implemented to alleviate this issue (Fig. 3E), analogous to using an internal standard to normalize two chromatograms relative to each other. The standard deviation of the background corrected baseline noise (after Savitzky-Golay smoothing) was calculated as a function of a normalization factor (N_f) applied using the region between 6 and 7 min, selected because no peaks eluted after ~ 6 min, except for solvent peak at 10 min. The optimal N_f is a multiplication factor that accounts for the amplitude difference between the back-

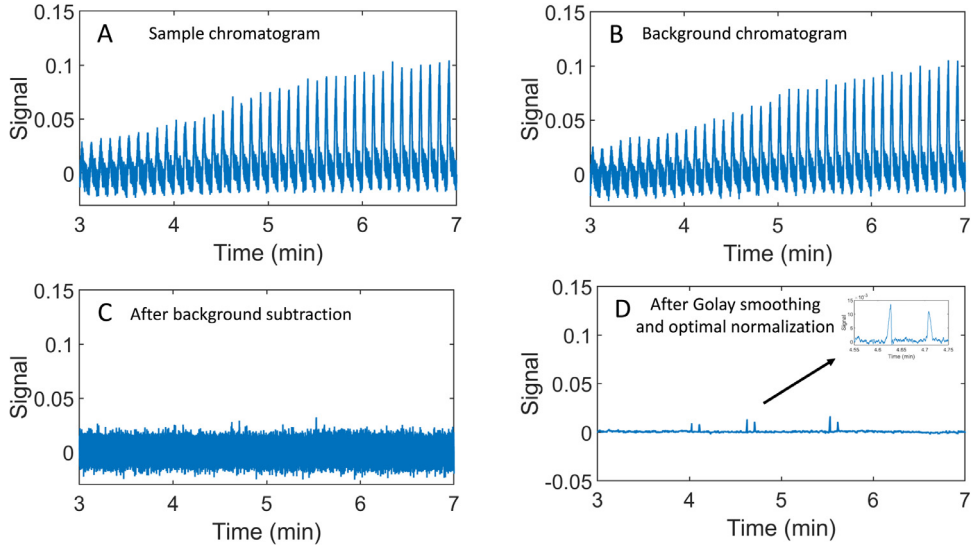

Fig. 4. (A) Raw modulated chromatogram of the 31-ppm alkane standard solution: (1) pentane, (2) hexane and (3) heptane. (B) Raw background chromatogram (no analyte injected). (C) Chromatogram after the background subtraction step. (D) Chromatogram after the Savitzky-Golay smoothing step when an optimized normalization factor (N_f = 1.02) is used. The insert shows the zoomed-in version of the two modulated ^{2}D hexane peaks.

ground noise in the sample chromatogram and the background chromatogram, that for a given background chromatogram produced the lowest standard deviation of the background corrected sample chromatogram (following the smoothing of the baseline noise). For the three lowest concentrations (7.8 ppm – 31.3 ppm) the optimal N_f ranged from 0.90 to 1.02. For the 500-ppm alkane standard solution, after background normalization is performed, N_f = 1.02 was found to be optimal, which when applied produced a flatter baseline in Fig. 3F.

While the relatively high concentration of the 500-ppm alkane standard solution is well suited for illustrating the baseline correction method in a stepwise manner, examination of a 31-ppm alkane standard solution chromatogram highlights the importance of the data processing for improving detectability. In Fig. 4A, the raw data collected for the 31-ppm standard solution does not appear to contain any analyte signal from the three alkanes, and visually appears similar to the background collected (Fig. 4B). After the background chromatogram is optimally normalized and then subtracted from 31-ppm standard solution chromatogram in Fig. 4A, analyte signal still cannot be distinguished from the baseline noise (Fig. 4C). However, after applying Savitzky-Golay smoothing, all three analytes are visible in the resulting chromatogram (Fig. 4D); for example, the two ^{2}D hexane peaks, obtained from modulation from ^{1}D to ^{2}D, are readily observed demonstrating the improved detectability (Fig. 4D insert).

To further illustrate the impact of using the normalization step during background correction (Fig. 3E), the overlay of 11 N_f's ±10% from N_f = 1 (by steps of 0.02) applied to 31-ppm standard solution data are shown in Fig. 5. Fig. 5A demonstrates how a baseline noise section (after background correction) changes depending upon the N_f applied, with the lowest (N_f = 0.9) producing the top blue curve and the highest (N_f = 1.1) producing the bottom purple curve. The original baseline section (N_f = 1) is highlighted in black, and the optimized background corrected baseline section (N_f = 1.02) is highlighted in green. The same color scheme was used in Fig. 5B, where the section of the chromatographic data containing the two ^{2}D hexane peaks observed (Fig. 4D insert) are background corrected as a function of N_f. The importance of proper normalization is critical for peak quantification, as a non-optimal N_f can not only bias peak height and area, but also broaden and distort the peak shapes, which impacts the quality of the overall 2D chromatogram obtained. The reproducibility achieved by the baseline correction method is illustrated in Fig. 5C, with overlays of the four 31-ppm standard solution replicates after the optimal N_f (ranging from 1.00 to 1.02) is applied (shifted vertically and left to right for clarity). Finally, the unfolded vector chromatograms from Fig. 5C were reshaped into 2D plots of the GC × GC chromatograms, and following ^{2}D alignment, summed along ^{1}D to produce a single ^{2}D peak per analyte, with the results for the four replicates of the 31-ppm and 7.8-ppm hexane peaks presented in Fig. 5D plotted along the ^{2}D time axis. Excellent reproducibility in peak height and peak width is observed.

These summed ^{2}D peaks (as in Fig. 5D) were used to recreate the unmodulated peak for easier area quantification, and to produce calibration curves for each analyte, with the calibration curves for hexane provided in Fig. 6A, B. The full concentration range of 7.8 ppm–4000 ppm was examined, and a linear relationship observed (r^2 > 0.999) in Fig. 6A. Further, Fig. 6B more clearly shows the calibration data for the low concentration range of 7.8 ppm–31.3 ppm. Each data point on the calibration curves shows the average and standard deviation among four replicates, albeit the standard deviation was smaller than the dot plotted for most of the concentration levels. The corresponding calibration curves for pentane and heptane were also prepared (not shown for brevity); these analytes also exhibit linear relationships (r^2 > 0.991). Using the summed ^{2}D peak areas of the 7.8-ppm standard solution data, as shown in blue in Fig. 5D for hexane, the limit-of-detection (*LOD*) and limit-of-quantification (*LOQ*) metrics were calculated for the three alkanes in the standard solution. Hexane exhibited the best detection sensitivity, the *LOD* was 0.9 ppm, with a *LOQ* of 3.0 ppm. For pentane, the *LOD* was 2.5 ppm with a *LOQ* of 8.2 ppm. Finally, the *LOD* of heptane was determined to be 1.9 ppm, with a *LOQ* of 6.4 ppm. It is important to note that these *LOD* and *LOQ* values would have been biased and inflated if the normalization factor step shown in Fig. 3E was not used. The peak areas are bigger or smaller when normalization is not used (N_f = 1) as in Fig. 6C; the standard deviation is much higher at the lowest three concentrations compared to when the optimal N_f is used in Fig. 6B.

The benefit of using normalization is further seen by comparing the percent deviation (% deviation) in the peak area in Fig. 6D, between when N_f = 1 is used (Fig. 6C) (in other words, when

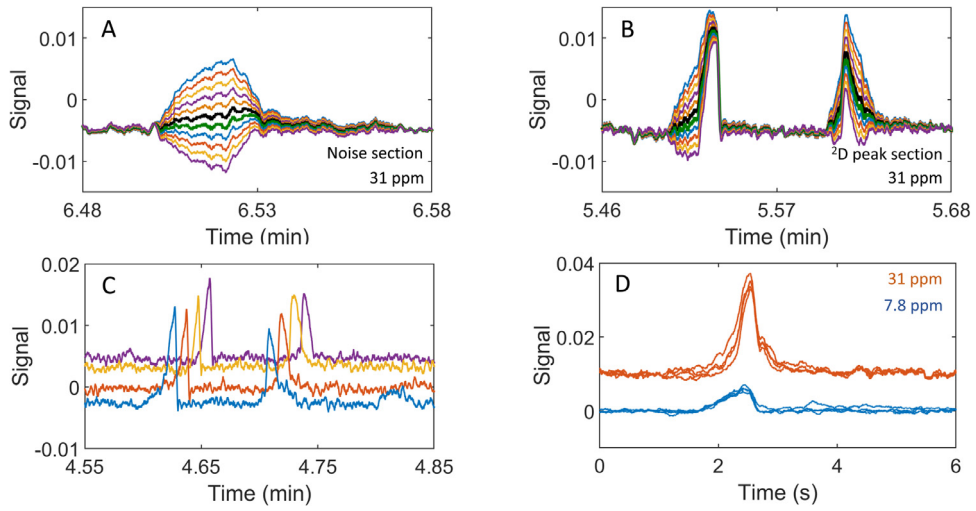

Fig. 5. Overlay of processed vector chromatograms of 31-ppm alkane standard solution produced using different normalization factors (±10% from $N_f = 1$), where black line represents using $N_f = 1$, and green line represents using the optimal $N_f = 1.02$. (A) Baseline noise section (no analytes eluting). (B) Section of the data where hexane ^{2}D peaks elute. (C) Unfolded data of 31-ppm hexane standard solution for 4 replicates, after data processing using an optimized N_f ranging from 1.00 to 1.02. (D) Summed ^{2}D hexane peaks obtained by summing along ^{1}D for 4 replicates at 31 and 7.8 ppm.

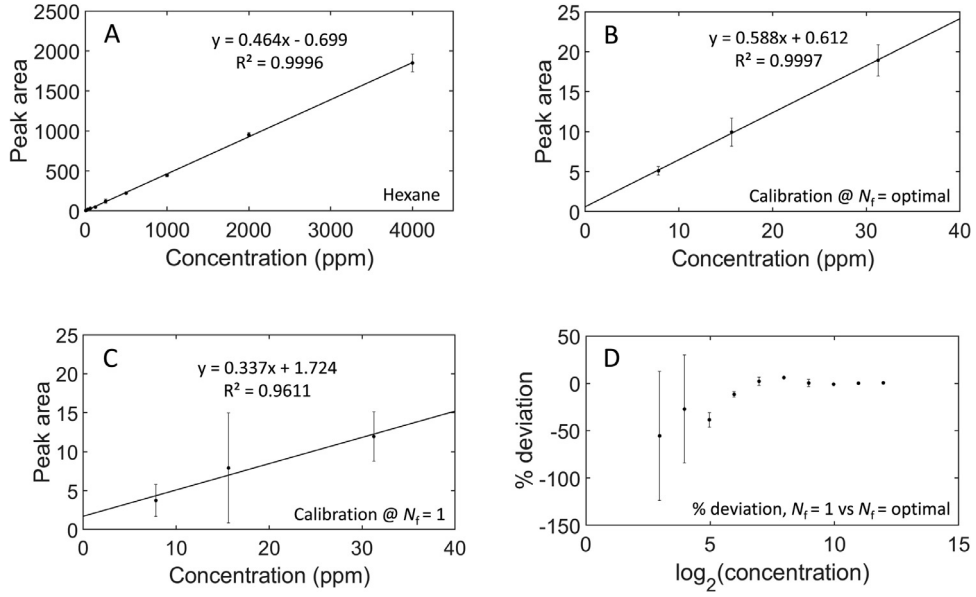

Fig. 6. (A) Peak area versus concentration calibration plot for hexane (7.8 ppm–4000 ppm). Peak areas measured from summed ^{2}D peaks as in Fig. 5D. Calibration plots for lowest three concentrations (7.8 ppm, 15.6 ppm, 31.3 ppm) with optimal N_f (B) and with $N_f = 1$ (C). (D) Percent deviation (% deviation) between peak areas obtained when N_f = optimal and when $N_f = 1$ for the full concentration range 7.8 ppm – 4000 ppm on a $\log_2$ concentration scale.

normalization step is omitted), and when N_f = optimal is used (Fig. 6B). Here the % deviation at a given standard concentration is defined as the peak area obtained from an optimally normalized peak area (optimal N_f) subtracted from the peak area at $N_f = 1$ (Fig. 6C) divided by the peak area obtained from optimally normalized peak area, then multiplied by 100 %, averaged for the replicates. The % deviation is smaller (essentially 0%) at higher concentrations but is substantially less at 15.6 and 7.8 ppm when background normalization is applied. Indeed, when background normalization is omitted ($N_f = 1$), the areas obtained varied by as much as 120%. Based on the results from Fig. 6 we conclude that the background normalization correction improved analyte detectability, which in turn benefits the *LOD* and *LOQ*. However, the intent of this work is not to compare the *LOD* and *LOQ* obtained to other methods, rather to improve the performance of DPGM-GC × GC-FID.

A separation of a natural gas sample in Fig. 7 illustrates the efficacy of the baseline correction method for a real sample. Since natural gas is a combination of mostly methane, with only small amounts of other volatile hydrocarbons, accurate trace analysis benefits greatly from the method. The GC × GC-FID data in unfolded vector form of the natural gas sample after application of the method is shown in Fig. 7A, where all the hydrocarbons have baseline resolution including the butane and pentane isomers. Application of the method allows for detection of both isopentane and n-pentane, that each compose only 1% of the natural gas sample. The folded GC × GC-FID chromatogram (Fig. 7B) provides adequate separation of these C1-C5 alkanes along ^{1}D, while on ^{2}D they are minimally retained. However, and more importantly, application of DPGM-GC × GC-FID provides 100% duty cycle modulation, resulting in appreciable detection sensitivity enhancement for

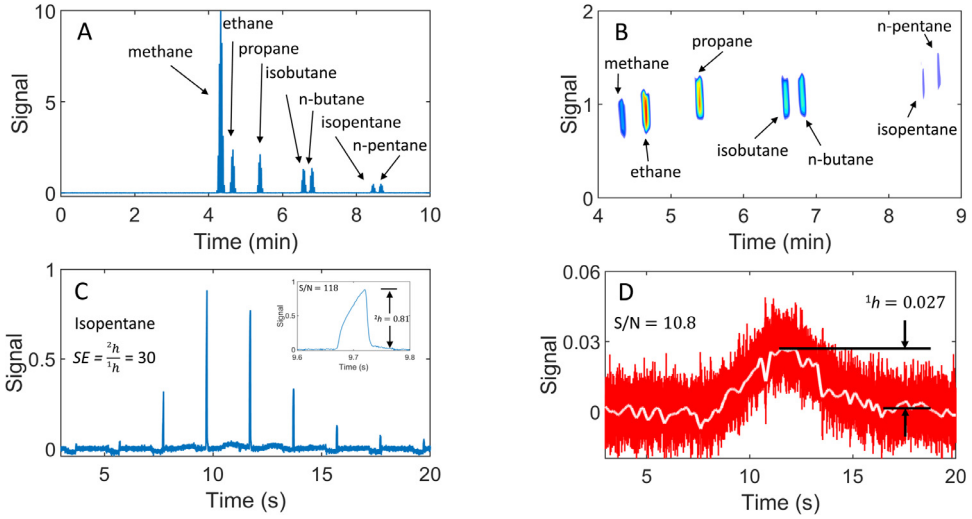

Fig. 7. Analysis of a natural gas sample. (A) Unfolded vector form chromatogram of a natural gas sample separation, following the baseline correction method, showing full separation of light hydrocarbons in the sample. (B) Processed GC × GC chromatogram that has made from (A) by folding the data at the P_M. Methane peak was purposely plotted on a 10-fold less sensitive scale, to more accurately reveal less concentrated peaks in the sample. (C) The modulated isopentane ^{2}D peaks with the signal enhancement (*SE*) calculation illustrated. The insert shows the zoom-in of the tallest ^{2}D peak. (D) Unmodulated isopentane ^{1}D peak (red) with a white trace showing the unmodulated peak that has been boxcar averaged to contain the same number of data points as the tallest modulated ^{2}D peak in (C). In both (C) and (D) the retention times shown are relative; the pentane peak in (C) elutes about 2 min later than in (D).

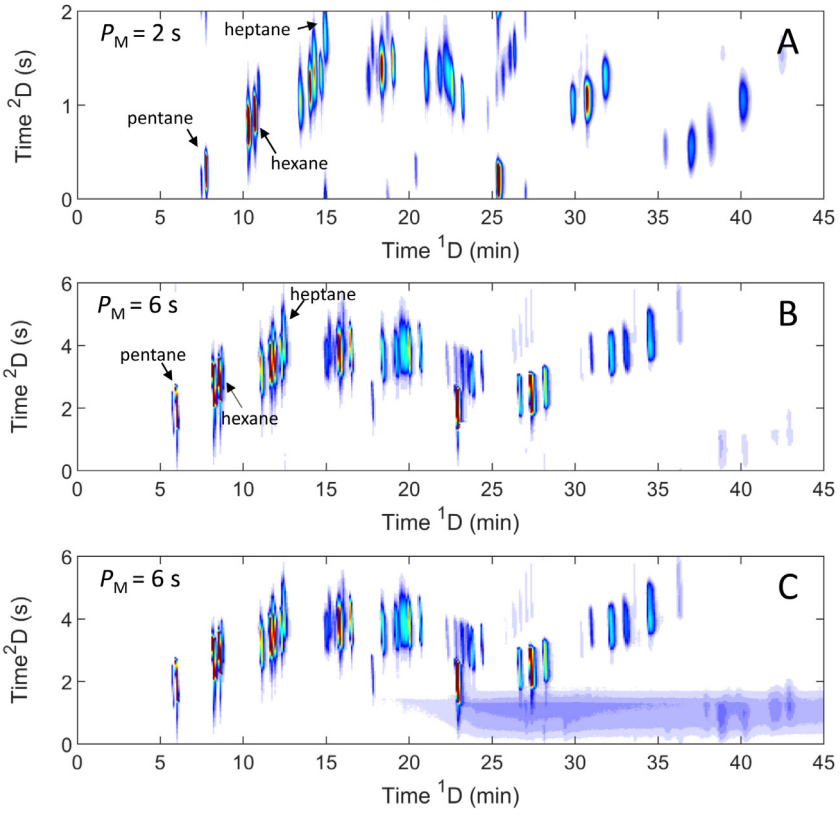

Fig. 8. Analysis of an unleaded gasoline sample. GC × GC chromatograms are produced for the separation at (A) P_M = 2 s, p_w = 0.5 s and (B) P_M = 6 s, p_w = 2 s, with the baseline correction method applied in both cases. (C) GC × GC chromatogram is produced for the separation at P_M = 6 s, p_w = 2 s without applying the baseline correction method. After 25 min, darker feature is due to the baseline noise.

the analysis of the low concentration analytes in the natural gas sample (Fig. 7C, D). The signal enhancement (*SE*) is calculated by dividing the height of the tallest ^{2}D peak in the modulated chromatogram for the analyte by the height of the unmodulated ^{1}D peak [18–20,41], providing a *SE* of 30 for isopentane (Fig. 7C, D), as the ^{1}D peak width-at-base is about 10 s, modulated about 5 times (with P_M = 2 s) into ^{2}D peaks with a width-at-base of 70 ms. This is particularly important for isopentane and n-pentane, as these analytes present in the natural gas sample have been known to be difficult to quantify due to their low concentration and low *S/N* [10]. Indeed, the tallest modulated isopentane ^{2}D peaks (Fig. 7C insert) has an 11-fold higher *S/N* than the boxcar averaged unmodulated ^{1}D peak (Fig. 7D white trace) for isopentane (resampled to have the same number of data points for an objective comparison).

Additionally, we confirmed that the total peak area of the modulated ^{2}D peaks was equal to the area of the ^{1}D peak (within 3%), confirming 100% duty cycle.

The DPGM-GC × GC-FID chromatograms of the unleaded gasoline sample analyzed with P_M = 2 s and P_M = 6 s (after applying the method) and P_M = 6 s (without applying the method) are provided in Fig. 8A–C, respectively, to provide an example of a complex sample analyzed with the baseline correction method in which several of the analyte peaks are not baseline resolved. The two modulation periods produced similar 2D peak capacities (Fig. 8A, B): $n_{c,2D}$ = 231 for P_M = 2 s, and $n_{c,2D}$ = 250 for P_M = 6 s. Although the ^{1}D peak widths on average were nearly identical, the average ^{2}D peak widths were found to be proportionate to the modulation period: ^1W_b = 26 s and ^2W_b = 0.8 s for P_M = 2 s, and ^1W_b = 24 s and ^2W_b = 2.4 s for P_M = 6 s. Although it is not obvious in the separations, a P_M = 6 s avoided most of the wraparound of the ^{2}D separations, while the P_M = 2 s allowed the ^{2}D separations to wrap around a couple times. The longer modulation period of P_M = 6 s provided a shorter ^{1}D run time, which is a consequence of the stop-flow nature of applying DPGM. More modulations per ^{1}D run time slows that separation to a greater extent. Pentane, hexane, and heptane were identified by retention time comparison to the injection of a standard solution and are labeled accordingly in Fig. 8A, B. Without application of the data analysis method to remove the background noise, the smaller, less concentrated peaks that appear in the chromatogram after 25 min would not be visible (Fig. 8C), which highlights the importance of the baseline correction method for complex samples. It also means that the data processing has the most impact on the compounds that elute at high temperature and are unretained on the second dimension (Fig. 8 B, C).

4. Conclusion

A baseline correction method for DPGM-GC × GC-FID analysis of trace level VOCs has been presented. Method development was demonstrated via analysis of alkane standard solutions (containing pentane, hexane, and heptane) and obtained linear calibration curves (r^2 > 0.991) for the three compounds. *LOD* and *LOQ* metrics were calculated for pentane (*LOD* = 2.5 ppm, *LOQ* = 8.2 ppm), hexane (*LOD* = 0.9 ppm, *LOQ* = 3.0 ppm), and heptane (*LOD* = 1.9 ppm, *LOQ* = 6.4 ppm). Analysis of a natural gas sample examined the utility of the overall instrumental and data analysis method for analytes below C6. Key analytes in the natural gas sample were baseline separated, whereby the *S/N* for isopentane increased 11-fold with an *SE* of 30. Improved detection sensitivity is also demonstrated for a gasoline sample, where a much cleaner GC × GC-FID chromatogram is obtained after the baseline correction method is applied. Future work on optimizing instrumental design to gain the ability to obtain background and sample chromatograms at the same time could in principle be performed. However, our experience was that by collecting a representative background chromatogram once per day, that the other sample chromatograms could be adequately corrected by the method presented. Thus, the method broadens the scope and utility of DPGM-GC × GC-FID to trace analysis applications.

Funding

This research did not receive any specific grant from funding agencies in the public, commercial, or not-for-profit sectors.

Declaration of Competing Interest

None.

CRediT authorship contribution statement

Lina Mikaliunaite: Conceptualization, Formal analysis, Investigation, Methodology, Resources, Validation, Visualization, Writing - original draft, Writing - review & editing. **Paige E. Sudol:** Conceptualization, Data curation, Investigation, Methodology. **Caitlin N. Cain:** Conceptualization, Data curation, Investigation. **Robert E. Synovec:** Conceptualization, Investigation, Methodology, Funding acquisition, Project administration, Resources, Supervision, Writing - review & editing.

References

[1] V.I. Safarova, S.V. Sapelnikova, E.V. Djazhenko, G.I. Teplova, G.F. Shajdulina, F.K. Kudasheva, Gas chromatography-mass spectrometry with headspace for the analysis of volatile organic compounds in waste water, J. Chromatogr. B 800 (2004) 325–330, doi:10.1016/j.jchromb.2003.10.070.

[2] C.V. Antoniou, E.E. Koukouraki, E. Diamadopoulos, Determination of chlorinated volatile organic compounds in water and municipal wastewater using headspace-solid phase microextraction-gas chromatography, J. Chromatogr. A 1132 (2006) 310–314, doi:10.1016/j.chroma.2006.08.082.

[3] C. Brasseur, J. Dekeirsschieter, E.M.J. Schotsmans, S. de Koning, A.S. Wilson, E. Haubruge, J.-F. Focant, Comprehensive two-dimensional gas chromatography-time-of-flight mass spectrometry for the forensic study of cadaveric volatile organic compounds released in soil by buried decaying pig carcasses, J. Chromatogr. A 1255 (2012) 163–170, doi:10.1016/j.chroma.2012.03.048.

[4] A. Serrano, M. Gallego, Sorption study of 25 volatile organic compounds in several mediterranean soils using headspace-gas chromatography-mass spectrometry, J. Chromatogr. A 1118 (2006) 261–270, doi:10.1016/j.chroma.2006.03.095.

[5] S.A. Baylis, K. Hall, E.J. Jumeau, The analysis of the C_1-C_5 components of natural gas samples using gas chromatography-combustion-isotope ratio mass spectrometry, Org. Geochem. 21 (1994) 777–785, doi:10.1016/0146-6380(94)90019-1.

[6] L.S. Moreira, L.A. d'Avila, D.A. Azevedo, Automotive gasoline quality analysis by gas chromatography: study of adulteration, Chromatographia 58 (2003) 501–505, doi:10.1365/s10337-003-0065-z.

[7] P. Doble, M. Sandercock, E. Du Pasquier, P. Petocz, C. Roux, M. Dawson, Classification of premium and regular gasoline by gas chromatography/mass spectrometry, principal component analysis and artificial neural networks, Forensic Sci. Int. 132 (2003) 26–39, doi:10.1016/S0379-0738(03)00002-1.

[8] P.E. Sudol, K.M. Pierce, S.E. Prebihalo, K.J. Skogerboe, B.W. Wright, R.E. Synovec, Development of gas chromatographic pattern recognition and classification tools for compliance and forensic analyses of fuels: a review, Anal. Chim. Acta 1132 (2020) 157–186, doi:10.1016/j.aca.2020.07.027.

[9] L. Bai, J. Smuts, P. Walsh, H. Fan, Z. Hildenbrand, D. Wong, D. Wetz, K.A. Schug, Permanent gas analysis using gas chromatography with vacuum ultraviolet detection, J. Chromatogr. A 1388 (2015) 244–250, doi:10.1016/j.chroma.2015.02.007.

[10] A.S. Brown, M.J.T. Milton, C.J. Cowper, G.D. Squire, W. Bremser, R.W. Branch, Analysis of natural gas by gas chromatography: reduction of correlated uncertainties by normalisation, J. Chromatogr. A 1040 (2004) 215–225, doi:10.1016/j.chroma.2004.04.007.

[11] M.A. Buldakov, V.A. Korolkov, I.I. Matrosov, D.V. Petrov, A.A. Tikhomirov, B.V. Korolev, Analyzing natural gas by spontaneous Raman scattering spectroscopy, J. Opt. Technol. 80 (2013) 426–430, doi:10.1364/JOT.80.000426.

[12] A. Petculescu, R.M. Lueptow, Quantitative acoustic relaxational spectroscopy for real-time monitoring of natural gas: a perspective on its potential, Sens. Actuator B Chem. 169 (2012) 121–127, doi:10.1016/j.snb.2012.03.086.

[13] M.M. Rahman, A.M.A. El-Aty, J.-H. Choi, H.-C. Shin, S.C. Shin, J.-H. Shim, Basic overview on gas chromatography columns, in: Analytical Separation Science, American Cancer Society, 2015, pp. 823–834, doi:10.1002/9783527678129.assep024.

[14] D. Bennett, Analysis of gas mixtures by gas chromatography, J. Chromatogr. A 26 (1967) 482–484, doi:10.1016/S0021-9673(01)98907-1.

[15] J.S. Stufkens, H.J. Bogaard, Rapid method for the determination of the composition of natural gas by gas chromatography, Anal. Chem. 47 (1975) 383–386, doi:10.1021/ac60353a060.

[16] R. Gras, J. Luong, V. Carter, L. Sieben, H. Cortes, Practical method for the measurement of Alkyl mercaptans in natural gas by multi-dimensional gas chromatography, capillary flow technology, and flame ionization detection, J. Chromatogr. A 1216 (2009) 2776–2782, doi:10.1016/j.chroma.2008.09.029.

[17] J.L. Burger, T.M. Lovestead, T.J. Bruno, Composition of the C_6+ fraction of natural gas by multiple porous layer open tubular capillaries maintained at low temperatures, Energy Fuel. 30 (2016) 2119–2126, doi:10.1021/acs.energyfuels.6b00043.

[18] J. Krupčík, P. Májek, R. Gorovenko, I. Špánik, P. Sandra, D.W. Armstrong, On the determination of a detector response enhancement factor for flow modulated comprehensive two-dimensional gas chromatography, J. Chromatogr. A 1286 (2013) 235–240, doi:10.1016/j.chroma.2013.02.068.

[19] T.J. Trinklein, S. Schöneich, P.E. Sudol, C.G. Warren, D.V. Gough, R.E. Synovec, Total-transfer comprehensive three-dimensional gas chromatography with time-of-flight mass spectrometry, J. Chromatogr. A 1634 (2020) 461654, doi:10.1016/j.chroma.2020.461654.
[20] A.L. Lee, K.D. Bartle, A.C. Lewis, A model of peak amplitude enhancement in orthogonal two-dimensional gas chromatography, Anal. Chem. 73 (2001) 1330–1335, doi:10.1021/ac001120s.
[21] Z. Liu, J.B. Phillips, Comprehensive two-dimensional gas chromatography using an on-column thermal modulator interface, J. Chromatogr. Sci. 29 (1991) 227–231, doi:10.1093/chromsci/29.6.227.
[22] B. Gruber, B.A. Weggler, R. Jaramillo, K.A. Murrell, P.K. Piotrowski, F.L. Dorman, Comprehensive two-dimensional gas chromatography in forensic science: A critical review of recent trends, TrAC Trends Anal. Chem. 105 (2018) 292–301, doi:10.1016/j.trac.2018.05.017.
[23] H.P. Tan, T.S. Wan, C.L.S. Min, M. Osborne, K.H. Ng, Quantitative analysis of fragrance in selectable one dimensional or two dimensional gas chromatography-mass spectrometry with simultaneous detection of multiple detectors in single injection, J. Chromatogr. A 1333 (2014) 106–115, doi:10.1016/j.chroma.2014.01.073.
[24] L. Mondello, A. Casilli, P.Q. Tranchida, G. Dugo, P. Dugo, Comprehensive two-dimensional gas chromatography in combination with rapid scanning quadrupole mass spectrometry in perfume analysis, J. Chromatogr. A 1067 (2005) 235–243, doi:10.1016/j.chroma.2004.09.040.
[25] E. Skoczyńska, P. Korytár, J. de Boer, Maximizing Chromatographic information from environmental extracts by GCxGC-ToF-MS, Environ. Sci. Technol. 42 (2008) 6611–6618, doi:10.1021/es703229t.
[26] L.R. Bordajandi, J.J. Ramos, J. Sanz, M.J. González, L. Ramos, Comprehensive two-dimensional gas chromatography in the screening of persistent organohalogenated pollutants in environmental samples, J. Chromatogr. A 1186 (2008) 312–324, doi:10.1016/j.chroma.2007.12.013.
[27] Y. Nolvachai, C. Kulsing, P.J. Marriott, Multidimensional gas chromatography in food analysis, TrAC Trends Anal. Chem. 96 (2017) 124–137, doi:10.1016/j.trac.2017.05.001.
[28] M. Edwards, A. Mostafa, T. Górecki, Modulation in comprehensive two-dimensional gas chromatography: 20 years of innovation, Anal. Bioanal. Chem. 401 (2011) 2335–2349, doi:10.1007/s00216-011-5100-6.
[29] H.D. Bahaghighat, C.E. Freye, R.E. Synovec, Recent advances in modulator technology for comprehensive two dimensional gas chromatography, TrAC Trends Anal. Chem. 113 (2019) 379–391, doi:10.1016/j.trac.2018.04.016.
[30] M.S. Klee, J. Cochran, M. Merrick, L.M. Blumberg, Evaluation of conditions of comprehensive two-dimensional gas chromatography that yield a near-theoretical maximum in peak capacity gain, J. Chromatogr. A 1383 (2015) 151–159, doi:10.1016/j.chroma.2015.01.031.
[31] J. Luong, X. Guan, S. Xu, R. Gras, R.A. Shellie, Thermal independent modulator for comprehensive two-dimensional gas chromatography, Anal. Chem. 88 (2016) 8428–8432, doi:10.1021/acs.analchem.6b02525.
[32] T. Hyötyläinen, M. Kallio, K. Hartonen, M. Jussila, S. Palonen, M.-L. Riekkola, Modulator design for comprehensive two-dimensional gas chromatography: quantitative analysis of polyaromatic hydrocarbons and polychlorinated biphenyls, Anal. Chem. 74 (2002) 4441–4446, doi:10.1021/ac0201528.
[33] A. Mostafa, T. Górecki, Development and design of a single-stage cryogenic modulator for comprehensive two-dimensional gas chromatography, Anal. Chem. 88 (2016) 5414–5423, doi:10.1021/acs.analchem.6b00767.
[34] V. Mucédola, L.C.S. Vieira, D. Pierone, A.L. Gobbi, R.J. Poppi, L.W. Hantao, Thermal desorption modulation for comprehensive two-dimensional gas chromatography using a simple and inexpensive segmented-loop fluidic interface, Talanta 164 (2017) 470–476, doi:10.1016/j.talanta.2016.12.005.
[35] W.-C. Liao, C.-F. Ou-Yang, C.-H. Wang, C.-C. Chang, J.-L. Wang, Two-dimensional gas chromatographic analysis of ambient light hydrocarbons, J. Chromatogr. A 1294 (2013) 122–129, doi:10.1016/j.chroma.2013.04.008.
[36] S.E. Prebihalo, K.L. Berrier, C.E. Freye, H.D. Bahaghighat, N.R. Moore, D.K. Pinkerton, R.E. Synovec, Multidimensional gas chromatography: advances in instrumentation, chemometrics, and applications, Anal. Chem. 90 (2018) 505–532, doi:10.1021/acs.analchem.7b04226.
[37] J.V. Seeley, F. Kramp, C.J. Hicks, Comprehensive two-dimensional gas chromatography via differential flow modulation, Anal. Chem. 72 (2000) 4346–4352, doi:10.1021/ac000249z.
[38] C.E. Freye, L. Mu, R.E. Synovec, High temperature diaphragm valve-based comprehensive two-dimensional gas chromatography, J. Chromatogr. A 1424 (2015) 127–133, doi:10.1016/j.chroma.2015.10.098.
[39] C.E. Freye, R.E. Synovec, High temperature diaphragm valve-based comprehensive two-dimensional gas chromatography with time-of-flight mass spectrometry, Talanta 161 (2016) 675–680, doi:10.1016/j.talanta.2016.09.002.
[40] C.E. Freye, H.D. Bahaghighat, R.E. Synovec, Comprehensive two-dimensional gas chromatography using partial modulation via a pulsed flow valve with a short modulation period, Talanta 177 (2018) 142–149, doi:10.1016/j.talanta.2017.08.095.
[41] T.J. Trinklein, D.V. Gough, C.G. Warren, G.S. Ochoa, R.E. Synovec, Dynamic pressure gradient modulation for comprehensive two-dimensional gas chromatography, J. Chromatogr. A 1609 (2020) 460488, doi:10.1016/j.chroma.2019.460488.
[42] S. Schöneich, D.V. Gough, T.J. Trinklein, R.E. Synovec, Dynamic pressure gradient modulation for comprehensive two-dimensional gas chromatography with time-of-flight mass spectrometry detection, J. Chromatogr. A 1620 (2020) 460982, doi:10.1016/j.chroma.2020.460982.
[43] S. Schöneich, T.J. Trinklein, C.G. Warren, R.E. Synovec, A systematic investigation of comprehensive two-dimensional gas chromatography time-of-flight mass spectrometry with dynamic pressure gradient modulation for high peak capacity separations, Anal. Chim. Acta 1134 (2020) 115–124, doi:10.1016/j.aca.2020.08.023.
[44] A.Y. Sholokhova, Y.V. Patrushev, V.N. Sidelnikov, A.K. Buryak, Analysis of light components in pyrolysis products by comprehensive two-dimensional gas chromatography with PLOT columns, Talanta 209 (2020) 120448, doi:10.1016/j.talanta.2019.120448.
[45] Y.V. Patrushev, V.N. Sidelnikov, Selection of the porous layer open tubular columns for separation of light components in comprehensive two-dimensional gas chromatography, J. Chromatogr. A 1579 (2018) 83–88, doi:10.1016/j.chroma.2018.10.015.
[46] C.A. Bruckner, B.J. Prazen, R.E. Synovec, Comprehensive two-dimensional high-speed gas chromatography with chemometric analysis, Anal. Chem. 70 (1998) 2796–2804, doi:10.1021/ac980164m.
[47] P.Q. Tranchida, S. Salivo, F.A. Franchina, L. Mondello, Flow-Modulated comprehensive two-dimensional gas chromatography combined with a high-resolution time-of-flight mass spectrometer: a proof-of-principle study, Anal. Chem. 87 (2015) 2925–2930, doi:10.1021/ac5044175.
[48] F. Stilo, E. Gabetti, C. Bicchi, A. Carretta, D. Peroni, S.E. Reichenbach, C. Cordero, J. McCurry, A step forward in the equivalence between thermal and differential-flow modulated comprehensive two-dimensional gas chromatography methods, J. Chromatogr. A 1627 (2020) 461396, doi:10.1016/j.chroma.2020.461396.
[49] N. Oldridge, O. Panic, T. Górecki, Stop-flow comprehensive two-dimensional gas chromatography with pneumatic switching, J. Sep. Sci. 31 (2008) 3375–3384, doi:10.1002/jssc.200800265.
[50] R.E. Mohler, B.J. Prazen, R.E. Synovec, Total-transfer, valve-based comprehensive two-dimensional gas chromatography, Anal. Chim. Acta 555 (2006) 68–74, doi:10.1016/j.aca.2005.08.072.
[51] X. Guan, J. Luong, Z. Yu, H. Jiang, Quasi-Stop-Flow modulation strategy for comprehensive two-dimensional gas chromatography, Anal. Chem. 92 (2020) 6251–6256, doi:10.1021/acs.analchem.0c00814.